International Archive of Applied Sciences and Technology, Vol 1 [2] December 2010: 62 - 70

ISSN 0976- 4828
http:// www.soeagra.com

RESEARCH ARTICLE

Calculation of Low Field Electron Transport Characteristics in Ge and Effects of Fast Neutron Radiation on its Crystal Structure

[1]H. Arabshahi and [2]F. Sarlak
[1]Department of Physics, Ferdowsi University of Mashhad, Mashhad, Iran
[2]Department of Physics, Payame Nour University of Fariman, Fariman, Iran
Email: fm_sarlak@yahoo.com

ABSTRACT
Temperature and doping dependencies of electron mobility in Ge crystal structure have been calculated using an iteravive technique. The following scattering mechanisims, i.e, impurity, polar optical phonon and acoustic phonon are inculded in the calculation. It is found that the electron mobility decreases monotonically as the temperature increases from 100K to 500K which is depended to the band structure characteristics of Ge. The low temperature value of electron mobilty increases significantly with increasing doping concentration. The amount of neutron energy deposition in Ge crystal of different sizes and at different distances from a neutron source has also been evaluated by using MCNP code. Then, the rate of atoms displacement in the crystals has been calculated using NRT Model. The damage to crystal is proportional to the energy deposition of neutron directly. Results show that number of atoms displacement in the crystal is related to the neutron radiation damage and increased by enlarging of crystal size.
***KEYWORDS**: Iteravive technique; ionized imurity scattering; neutron energy; crystal size; atom displacement.*

Introduction

Semiconductor detectors have high energy resolution and are used commonly for photon and charged particles spectroscopy. High pure Ge semiconductor is one of the best semiconductor detectors, which can be made in large size with a very suitable high energy resolution. Although, high pure Ge is very costly and must be kept at low temperature, it is widely used for gamma and x-ray spectroscopy [1-7]. When this crystal is located in a combined neutron-gamma field, neutron interactions with Ge element induce main crystal damages and distort its energy resolution [8]. Depending on the energy, neutron interactions with matter may undergo a variety of nuclear processes. The main interactions of fast neutrons are elastic scattering and inelastic scattering, but neutron capture is an important interaction for thermal neutrons [9]. Improved electron transport properties are one of the main targets in the ongoing study of semiconductor like Ge. The iterative technique has proved valuable for studying non-equilirium carrier transport in arange of semiconductor materials and devices [6-7]. However, carrier transport modeling of Ge material has only recently begun to receive sustained attention, now that the growth of compounds and alloys is able to produce valuable material for the electronics industry. In this communication we present iterative calculations of electron drift mobility in low electric field application. We demonstrate the effect of low electric field on the electron transport properties in these materials. The differences in transport properties are analyzed in terms of important material parameters. Most of the calculations have been carried out using a non-parabolic ellipsoidal valley model to describe transport in the conduction band. However, the simpler and less computationally intensive spherical parabolic band scheme has also been applied, to test the validity of this approximation. The iterative calculations take into account the electron-lattice interaction through polar optical phonon scattering and deformation potential acoustic phonon scattering (treated as an elastic process). Impurity scattering due to ionized and neutral donors is also included, with the latter found to be important at low temperature due to the relatively large donor binding energy which implies considerable carrier freeze-out already at liquid nitrogen tempearure.

We have also calculated neutron energy deposition on Ge crystal using MCNP code. We then evaluated the damage, the atom displacements rate of Ge crystal using NRT model. It is well known that the main damages of the crystal are atom displacements and neutron activation that varied for different neutron sources.

This paper is organised as follows. Details of the iterative model and the electron mobility calculations are presented in section II, the electron scattering mechanism which have been used are discussed in section III, the atom displacement model under high neutron energy deposition are explained in section IV and the results of calculations are interpreted in section V.

SIMULATION METHOD

In principle the iterative technique give exact numerical prediction of electron mobility in bulk semiconductors. To calculate mobility, we have to solve the Boltzmann equation to get the modified probability distribution function under the action of a steady electric field. Here, we have adopted the iterative technique for solving the Boltzmann transport equation. Under application of a uniform electric field the Boltzmann equation can be writte

$$(\frac{e}{\hbar})E.\nabla_k f = \oint [s' f'(1-f) - sf(1-f')]dk \qquad (1)$$

where $f = f(k)$ and $f' = f(k')$ are the probability distribution functions and $s = s(k,k')$ and $s' = s(k',k)$ are the differential scattering rates. If the electric field is small, we can treat the change from the equilibrium distribution function as a perturbation which is first order in the electric field. The distribution in the presence of a sufficiently small field can be written quite generally as

$$f(k) = f_0(k) + g(k)\cos\theta \qquad (2)$$

where $f_0(k)$ is the equilibrium distribution function, θ is the angle between k and E and $g(k)$ is an isotropic function of k, which is proportional to the magnitude of the electric field. In general, contributions to the differential scattering rates come from two types of scattering processes, elastic scattering s_{el}, due to acoustic, impurity, plasmon and piezoelectric phonons, and inelastic scattering s_{inel}, due to polar optic phonons

$$s(k,k') = s_{el}(k,k') + s_{inel}(k,k') \qquad (3)$$

Generally this scattering process can not be treated within the framework of the relaxation time approximation because of the possibility of the significant energy exchange between the electron and the polar optic modes. In this case, s_{inel} represents transitions from the state characterized by k to k' either by emission $[s_{em}(k,k')]$ or by absorption $[s_{ab}(k,k')]$ of a phonon. The total elastic scattering rate will be the sum of all the different scattering rates which are considered as elastic processes, i.e. acoustic, piezoelectric, ionized impurity, and electron-plasmon scattering. In the case of polar optic phonon scattering, we have to consider scattering-in rates by phonon emission and absorption as well as scattering-out rates by phonon absorption and emission. Using Boltzmann equation and considering all differential scattering rates, the factor $g(k)$ in the perturbed part of the distribution function $f(k)$ can be given by

$$g(k) = \frac{\frac{-eE}{\hbar}\frac{\partial f_0}{\partial k} + \sum\int g'\cos\varphi[s_{inel}'(1-f) + s_{inel} f)]dk}{\sum\int(1-\cos\varphi)s_{el}\,dk + \sum\int[s_{inel}(1-f') + s_{inel}' f']dk} \qquad (4)$$

Note, the first term in the denominator is simply the momentum relaxation rate for elastic scattering. It is interesting to note that if the initial distribution is chosen to be the equilibrium distribution, for which $g(k)$ is equal zero, we get the relaxation time approximation result after the first iteration. We have found that convergence can normally be achieved after only a few iterations for small electric fields. Once $g(k)$ has been evaluated to the required accuracy, it is possible to calculate quantities such as the drift mobility which is given by

$$\mu_d = \frac{\hbar}{3m} \frac{\int_0^\infty k^3 \frac{g(k)}{Ed} dk}{\int_0^\infty k^2 f(k) dk} \quad (5)$$

Where d is defined as $1/d = m\nabla_k E/\hbar^2 k$. In the following section electron-phonon, electron impurity and electron-plasmon scattering mechanisms will be discussed.

ELECTRON SCATTERING MECHANISMS

A. Phonon scatterin

The dominant scattering mechanism of electrons in polar semiconductors like Ge comes from the electron-phonon interaction except at the lowest temperatures. The electron-optical phonon interaction contributes both in the ohmic and non-ohmic mobility and provides the dominant energy-loss mechanism of electrons. First order polarization occurs in connection with the primitive unit cell, characteristic of the longitudinally polarized optical mode. In thesematerials the Debye temperature is more than 800K [6], hence polar optical phonon scattering must be considered as an inelastic process. Other phonon scattering processes, i.e. acoustic and piezoelectric scattering are considered as elastic processes. In polar optic phonon scattering the differential scattering rates for absorption and emission can be written as [5]

$$S_{op}(k,k') = \frac{\sqrt{2m^*}e^2\omega_{op}}{8\pi\varepsilon_0\hbar}\left(\frac{1}{\varepsilon_\infty} - \frac{1}{\varepsilon_s}\right) \frac{1+2\alpha E'}{\gamma^{1/2}(E)} F_0(E,E')\left\{N_{op}, (N_{op}+1)\right\} \quad (6)$$

where ε_s and ε_∞ are define in table 1, N_{op} is the phonon occupation number and the N_{op} and $1+N_{op}$ refer to absorption and emission, respectively. For small electric fields, the phonon population will be very close to equilibrium, so that the average number of phonons is given by the Bose-Einstein distribution function. We have found that after a few iterations, the electron polar optical phonon scattering rate converges and becomes very close to the experimental result [6]. The energy range involved in the case of scattering by acoustic phonons is from 0 to $2\hbar v_s k$, as the momentum conservation restricts the phonon wave vector q between 0 and 2k , where k is the electron wave vector. Typically the average value of k is on the order of 10^7 cm^{-1} and v_s, the velocity of sound in the medium, is on the order of 10^5 cm/s. Hence, $2\hbar v_s k \approx 1$ meV, which is small compared to the thermal energy. Hence electron-acoustic phonon scattering can be considered as an elastic process. Actually, a long wave length acoustic displacement can not affect the energy since neighboring unit cells move by almost the same amount, only the differential displacement (normally the strain) is of importance. The total differential scattering rate for acoustic phonons can be given by

$$S_{ac}(k,k') = \frac{\sqrt{2}D_{ac}^2 (m_t^* m_l^*)^{1/2} K_B T}{\pi\rho v^2 \hbar^4} \frac{\sqrt{E(1+\alpha E)}}{(1+2\alpha E)}\left[(1+\alpha E)^2 + 1/3(\alpha E)^2\right] \quad (7)$$

where D_{ac} is the acoustic deformation potential, ρ is the material density and α is the non-parabolicity coefficient. The formula clearly shows that the acoustic scattering increases with temperature.

B. Impurity scattering

The standard technique for dealing with ionized impurity scattering in semiconductors is the Brook-Herring (BH) technique [8], which is based on two inherent approximations. First, is the first order Born approximation and second is the single ion screening approximation. These two approximations essentially lead to a poor fit to the experimental mobility data [9,10]. Several attempts have been made to modify the BH technique phenomenologically [11]. It has been shown that phase-shift analysis of electron-impurity scattering is the best way to overcome the Born approximation. Departure from the BH prediction of electron mobility is evident at higher electron concentrations. Meyer and Bartoli [9] have provided an analytic treatment based on phase-shift analysis taking into account the multi-ion screening effect and finally been able to overcome both the approximations. All the previous techniques of impurity screening by free electrons in semiconductors were based on the Thomas-Fermi (TF) approximation which assures that a given impurity should be fully screened. The breakdown of the single-ion screening formalism becomes prominent in the strong screening regime, where the screening length calculated through TF theory becomes much shorter than the average distance between the impurities and hence neighboring potentials do not overlap significantly. This essentially leads to a physically unreasonable result. In the case of high compensation, the single-ion screening formalism becomes less relevant, because in order to maintain the charge neutrality condition, it would be more difficult for a given number of electrons to screen all the ionized donors separately. In the case of InP, the compensation ratio is usually quite large, and the ratio N_D^+/n is also temperature dependent. Hence the multi-ion screening correction is very essential in InP. The effective potential of an ionized impurity scattering center is spherically symmetric in nature, so one can use phase-shift analysis to find the differential scattering rate $s(k,k')$ more accurately. The effective potential $V(r)$ due to an ionized impurity can be expressed as $V(r)=-(Z_i e^2)/(4\pi\varepsilon_0\kappa_0 r)e^{-r/\lambda}$, where Z_i is the charge of the ionized impurity in units of e and λ is the screening length. The standard technique to find out the screening length is the TF approach which is based on single ion screening approximation. In TF one can calculate the charge contribution q_i to the screening of a single ionized donor by an electron of energy E_i and is given by $q_i=-(2e^3\lambda^2/\varepsilon_0\kappa_0 E_i V)$. In the case of multi-ion problem, the TF approach can be generalized to find out the effective charge contribution due to an electron to screen all ionized donors and can be given by $Q_i=-(2e^3 N_D^+\lambda^2/\varepsilon_0\kappa_0 E_i)$. Total screening charge exactly neutralizes the ionized donors, when Q_i is summed over all electronic states

$$\sum_i -\frac{Q_i}{e} f_0(E_i) = N_D^+ \tag{9}$$

For the sufficiently low energy electrons, Q_i can be greater than the electronic charge, which is physically unreasonable. One way to tackle [9] this problem is to introduce a factor S_i such that

$$S_i(E_i)=\frac{E_i}{\xi} \tag{10}$$

where $\xi=(2N_D^+c^2\lambda^2/\varepsilon_0 k_0)$, Q_i will be modified to $Q_i'=Q_i S_i$ in equation (9). For the low energy electrons the contribution will be –e. Since the total contribution to the screening by the low energy electrons has been effectively decreased, equation (9) no longer holds. However, if the screening length λ is more than the average distance between the donors, it is not necessary to insist that each donor be fully screened, only it is required that overall charge neutrality should be preserved. Electrons in the overlap region can provide screening to both the ionized donors. Here we can define a factor p, which would be the fraction of the total charge, which is contained within a sphere of radius R surrounding the donor. Hence equation (9) will be modified as

$$\sum_i -\frac{Q_i''}{e} f_0(E_i) = pN_D^+ \tag{11}$$

where $Q_i''=pQ_iS_i$. The screening charge requirement will be fulfilled by adjusting the screening length untill equation (11) is satisfied and is given by

$$\lambda_m^{-2}=\eta\lambda_0^{-2} \tag{12}$$

where λ_m is multi-ion screening length and λ_0 is TF screening length. The differential scattering rate for ionized impurity can be given as

$$S_{ii}(k,k') = \frac{8\pi^3\hbar^3}{m^{*2}V^2}\left|f(X)\right|^2\delta[E(k') - E(k)] \tag{13}$$

where scattering amplitude $f(X)$ depends on the phase shift δ_l and Legendre polynomial P_l and is given by

$$f(X) = \frac{1}{2ik}\sum_{l=0}^{\infty}(2l+1)(e^{2i\delta_l} - 1)P_l(X) \tag{14}$$

It has already been mentioned that in n-type Ge the activation energy of the donors is quite large, which keeps a large number of donors neutral at low temperatures. Neutral impurity scattering has been dealt with previously using the Erginsoy [12] expression which is based on electron scattering by a hydrogen atom and a scaling of the material parameters. It has been shown that an error as high as 45% results in the neutral impurity scattering cross section with this simple model. Meyer and Bartoli [9] have given a phase shift analysis treatment based on the variation results of Schwartz [12-19] to calculate the neutral impurity cross section, which is applicable for a larger range of electron energy.

THEORY OF ATOM DISPLACEMENT

A primary recoil atom is produced when an energetic incident particle such as fast neutron undergoes a collision with a lattice atom. If the energy transferred to the primary knock-on atom (PKA)is large enough, $E >> Ed$, (where Ed=30eV; the average energy for one displacement) [20], the PKA can continue the knock-on atom processes, producing secondary recoil atom displacements, which in turn can displace additional atoms. Such an event will result in many collision and displacement events occurring in near proximity of each other. The multiple displacement sequence of collision events is commonly referred to as a collision or displacement cascade [21]. Transferred energy to a PKA with atomic mass number A, when occurred and that a neutron of energy E recoiled, is given by

$$T = \frac{1}{2}\left(v_1^2 + v_0^2 + 2v_1v_0\cos\theta\right) = \frac{4AE}{(A+1)^2} \tag{15}$$

where v_1 is the velocity of scattering atom after collision, and v_0 is the centre of mass velocity. The original model for displacement damage, developed initially for simple metals, is due to Kinchin and Pease [22], and the standard formulation of it by Norgett *et al.* [23], often referred to as the NRT model, is

$$v(T) = \begin{cases} 0 & T \le E_d \\ 1 & E_d \le T \le 2E_d \\ 0.8T/2E_d & T \ge 2E_d \end{cases} \tag{16}$$

where $v(T)$ is the number of displaced atoms produced by a recoil atom of energy E and damage energy T, and E_d is the average threshold displacement energy for an atom in the crystal lattice. MCNP is a general-purpose Monte Carlo neutron, photon, and electron transport code. It has continuous-energy physics and is time-dependent. The geometry is any arbitrary configuration of three dimensional surfaces. It is used for radiation shielding, criticality safety, nuclear design, aerospace, medical, nonproliferation, radiation dose and other applications by several thousand users worldwide. This code is used to simulate one neutron at a time and records its history. The neutron energy deposition in the crystal has been calculated by tally F6:n for different neutron sources: mono-energy, Am-Be and ^{252}Cf sources [24].

CALCULATION RESULTS

We have performed a series of low-field electron mobility calculations in Ge material. Low-field mobility has been derived using iteration methode.

Figure 1 shows the calculated electron drift mobility in bulk Ge material as a function of temperature with free electron concentration of 10^{21} to 10^{23} m^{-3} and with the electric field applied along one of the cubic axes. It can be seen from the figure that the electron drift mobilities at room temperature that we find for Ge is 3000 cm^2/V-s at 10^{23} m^{-3} donor concentration. The results plotted in figure 1 indicate that the electron drift mobility of Ge is lower at donor concentration of 10^{23} m^{-3} at all temperatures. This is largely due to the higher electron scattering rate. Also it can be seen that below 100 K, ionized impurity scattering is the dominant forms of lattice scattering.

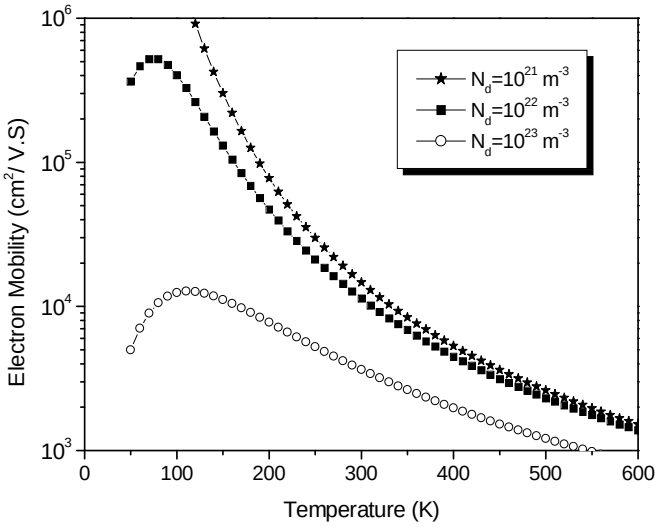

Fig 1. Electron drift mobility vs temperature of pure intrinsic Ge with free electron concentration up to10^{23} m^{-3}.

Figure 2 shows the calculated variation of the electron drift mobility as a function of free electron concentration for all crystal structures at temperatures up to 600 K. The mobility does not vary monotonically between free electron concentrations of 10^{20} m^{-3} and 10^{24} m^{-3} due to the dependence of electron scattering on free electron concentration, but shows a maximum near 10^{20} m^{-3} for all temperatures.

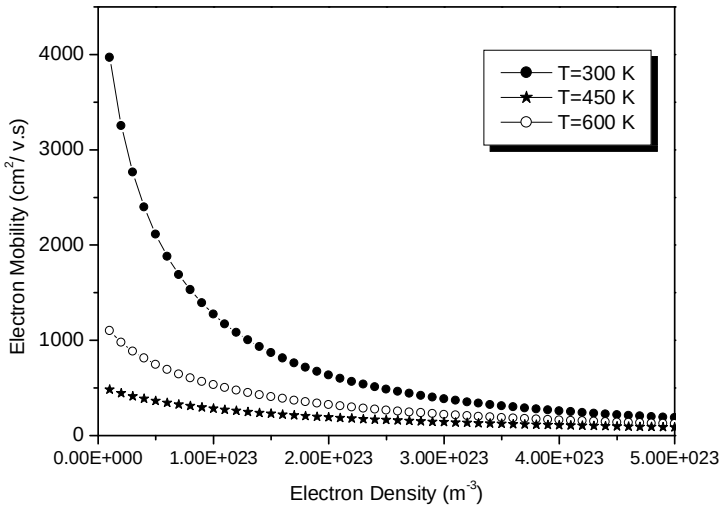

Fig 2. Calculated low-field electron drift mobility of Ge as a function of different free electron

concentration at temperature up to 600 K.

We have also calculated neutron energy deposition on Ge crystal using MCNP code. The Ge crystal is placed at different distances from point neutron sources with constant mono-energy and continuous energy spectrum such as Am-Be and ^{252}Cf source. Then, the amount of deposition energy per gram of crystal was calculated by F6:n tally of MCNP code. The amount of deposition energy per gram for different Ge crystal for Am-Be source as function of distance, per one neutron of source is illustrated in figure 3a. By using this data and the NRT model, the atom displacements rate for Ge crystals have been evaluated. These results are shown in figure 3b.

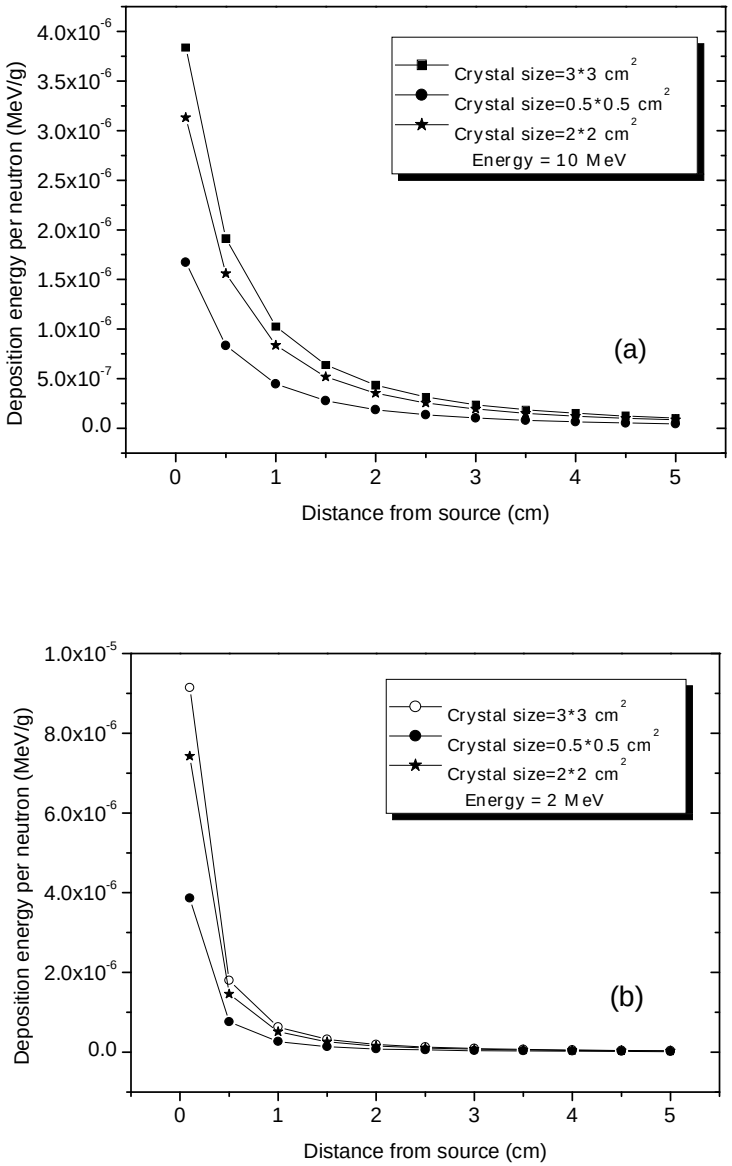

Figure 3: (a) Energy deposition per gram in different Ge crystal due to an Am-Be source; (b) the atom displacements rate.

The amount of deposition energy per gram in different Ge crystal size due to different mono energy rate in figure 3b has been shown. A comparison of atom displacements rate due function of distance

is illustrated in figure 4a and 4b shows the atom displacements rate placed on a point 2 MeV neutron source as a function of distance. The corresponding result for a ^{252}Cf source is shown figure 4a, and the atom displacements atom displacements rate in figure 4b. Energy deposition and corresponding atom displacements rate are decreases mostly by $1/r^2$ as we expected.
A comparison of atom displacements rate due to different sources located in 5 cm far from the crystal have been illustrated in figure 4. It can be seen that the neutron average energy of the source increases as well as the corresponding damage growing up.

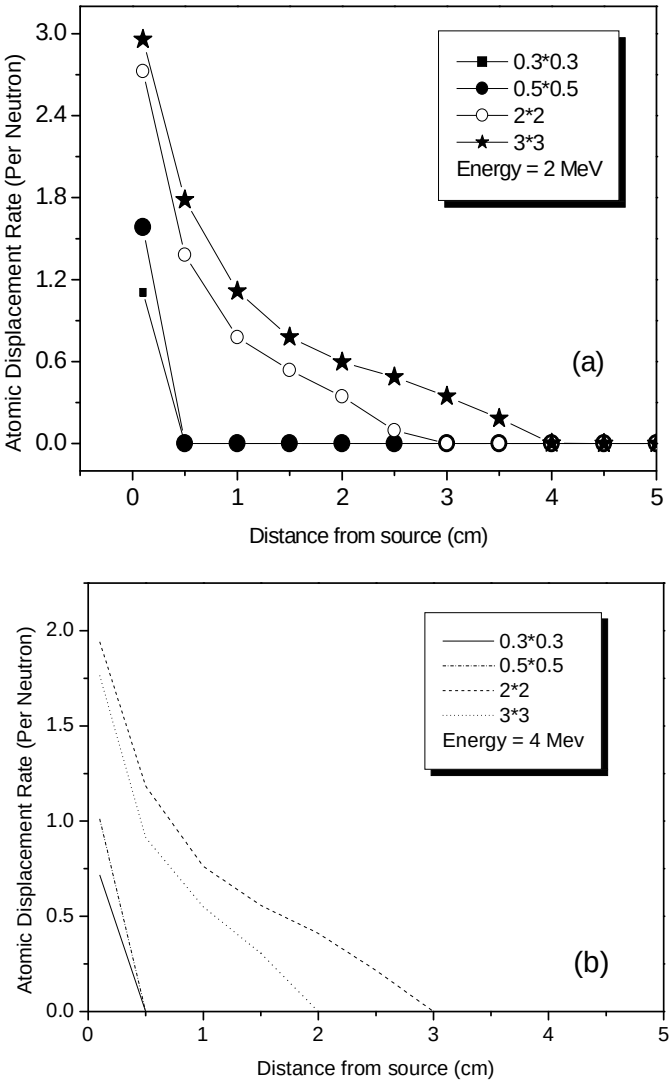

Figure 4: Comparison of atom displacements rate in Ge crystals that placed on 5 cm of different sources At different energy.

CONCLUSION

In conclusion, we have quantitatively obtained temperature-dependent and electron concentration-dependent electron mobility in Ge using an iteravive technique. The theoretical values show good agreement with recently obtained experimental data. Several scattering mechanisms have been included in the calculation. Ionized impurities have been treated beyond the Born approximation using a phase shift analysis. Screening of ionized impurities has been treated more realistically using a multi-ion screening formalism, which is more relevant in the case of highly compensated III-V semiconductors like GaAs. Our calculation results show also that the amount of deposition energy per gram of Ge crystals and total number of atom displacements are a function of crystal sizes. Collision

and displacement events occur more in larger crystal, because a neutron leaves crystal, after more collision. As well as, atom displacements increase when the energy of the source accrues. The amount of deposition energy per gram of crystal decreases if the distance between source and crystal get larger. It is because the reaction surface reduces than reaction volume.

REFERENCES

[1] S Nakamura, M Senoh and T Mukai, Appl. Phys. Lett. **62**, 2390 (1993)
[2] S Strite and H Morkoc, J. Vac. Sci. Technol. **B 10**, 1237 (1992).
[3] V W L Chin and T L Tansley, J. Appl. Phys. **75**, 7365 (1994).
[4] D L Rode and D K Gaskill, Appl. Phys. Lett. **66**, 1972 (1995).
[5] C Moglestue, *Monte Carlo simulation of semiconductor devices*, Chapman and Hall (1993).
[6] K T Tsen, D K Ferry, A Botchkarev, B Suerd, A Salvador and H Morkoc, Appl. Phys. Lett. **71**, 1852 (1997).
[7] B K Ridley, Electrons and phonons in semiconductor multilayers, Cambridge University press (1997)
[8] H Brooks, Phys. Rev. **83**, 879 (1951).
[9] J R Meyer and F J Bartoli, Phys. Rev. **B 23**, 5413 (1981).
[10] J R Meyer and F J Bartoli , *Solid State State* Commun. **41**, 19 (1982).
[11] D Chattopadhya and H J Queisser, *Rev. Mod. Phys.* **53**, 745 (1981).
[12] C Erginsoy, Phys. Rev. **79**, 1013 (1950).
[13] C Schwartz, Phys. Rev. **124**, 1468 (1961).
[14] M V Fischetti, Phys. Rev. **44**, 5527 (1991).
[15] H Morkoc, *Nitride semiconductor and devices*, Springer-velag (1999).
[16] Udayan, V Bhapkar and M S Shur, *J. Appl. Phys.* **82**,1649 (1997).
[17] R P Wang, P P Ruden, J Kolnik and K F Brennan, *Mat. Res. Soc. Symp. Proc.*, **445**, 935 (1997).
[18] J Ljungvall and J Nyberg, Nucl. Instr. Meth. Phys. Res. A **546**, 553 (2005).
[19] T Siiskonen and H Toivonen, Nucl. Instr. Meth. Phys. Res. A **504**, 403 (2005).
[20] H W Kraner, C Chasman and K W Jones, *Nucl. Instr. Meth. Phys. Res*. **62**, 173 (1968).
[21] N Fourches, A Huck and G Walter, *IEEE Trans. Nucl. Sci*. **38**, No. 3, 1728 (1991).
[22] L S Darken, Nucl. *Instr. Meth. Phys. Res*. B **74**, 523 (1993).
[23] J Llacer and H W Kraner, Nucl. *Instr. Meth. Phys. Res*. **98**, 467 (1972).
[24] L S Darken, R C Trammell, T W Raudorf, R. H. Pehl and J. H. Elliott. *Nucl. Instr. Meth. Phys. Res.* **171**, 49 (1980).